Inorganic Chemistry

Article

pubs.acs.org/IC

Expansion of the Rich Structures and Magnetic Properties of Neptunium Selenites: Soft Ferromagnetism in $Np(SeO_3)_2$

Kariem Diefenbach, Jian Lin, Justin N. Cross, Naresh S. Dalal, Michael Shatruk, and Thomas E. Albrecht-Schmitt*

Department of Chemistry and Biochemistry, Florida State University, 95 Chieftan Way, 310 DLC, Tallahassee, Florida 32306, United States

Supporting Information

ABSTRACT: Two new neptunium selenites with different oxidation states of the metal centers, $Np^{IV}(SeO_3)_2$ and $Np^{VI}O_2(SeO_3)$, have been synthesized under mild hydrothermal conditions at 200 °C from the reactions of NpO_2 and SeO_2. $Np(SeO_3)_2$ crystallizes as brown prisms (space group $P2_1/n$, a = 7.0089(5) Å, b = 10.5827(8) Å, c = 7.3316(5) Å, β = 106.953(1)°); whereas $NpO_2(SeO_3)$ crystals are garnet-colored with an acicular habit (space group $P2_1/m$, a = 4.2501(3) Å, b = 9.2223(7) Å, c = 5.3840(4) Å, β = 90.043(2)°). Single-crystal X-ray diffraction studies reveal that the structure of $Np(SeO_3)_2$ features a three-dimensional (3D) framework consisting of edge-sharing NpO_8 units that form chains that are linked via SeO_3 units to create a 3D framework. $NpO_2(SeO_3)$ possesses a lamellar structure in which each layer is composed of NpO_8 hexagonal bipyramids bridged via SeO_3^{2-} anions. Bond-valence sum calculations and UV-vis-NIR absorption spectra support the assignment of tetravalent and hexavalent states of neptunium in $Np(SeO_3)_2$ and $NpO_2(SeO_3)$, respectively. Magnetic susceptibility data for $Np(SeO_3)_2$ deviates substantially from typical Curie–Weiss behavior, which can be explained by large temperature-independent paramagnetic (TIP) effects. The Np^{IV} selenite shows weak ferromagnetic ordering at 3.1(1) K with no detectable hysteresis, suggesting soft ferromagnetic behavior.

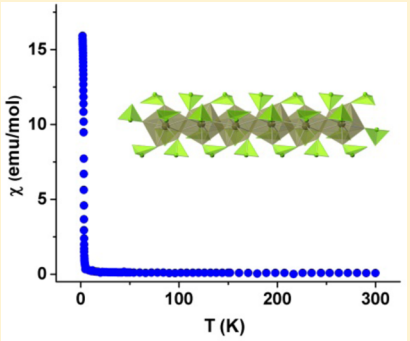

INTRODUCTION

The solid-state chemistry of neptunium is rich, which, in part, is due to the wide range of oxidation states that can be stabilized.[1] Well-characterized examples of Np^{III}, Np^{IV}, Np^{V}, Np^{VI}, and Np^{VII} compounds have been reported, with Np^{V} species dominating this chemistry, because of the stability of this state, with respect to disproportionation.[2] Neptunium in the penta- and hexavalent states adopts highly anisotropic coordination geometries, primarily because of the tendency for forming the linear dioxo neptunyl ions, NpO_2^{n+} (n = 1 or 2). These moieties are further coordinated by four to six additional donor atoms in a plane perpendicular to the neptunyl axis, yielding tetragonal, pentagonal, and hexagonal bipyramidal environments around the neptunium centers.[3] The geometries exhibited by the trivalent and tetravalent oxidation states are substantially different from the aforementioned ones, and these ions are typically found in eight- and nine-coordinate environments with a variety of distortions of dodecahedra (CN = 8) and tricapped trigonal prisms (CN = 9).[4] The eight-coordinate neptunium centers are particularly complex, because cubic (O_h),[5] trigonal dodecahedral (D_{2d}),[4a] bicapped trigonal prismatic (C_{2v}),[6] and square antiprismatic (D_{4d})[4a] all occur.

Each of the oxidation states of neptunium is capable of yielding magnetic behavior worthy of extensive probing. Np^{III}, which is the most challenging form, from a chemical manipulation standpoint, has expanded 5f and 6d orbitals, and mixing with ligand orbitals has pronounced effects on its electronic structure.[7] Np^{V}, while anticipated as being an uninteresting nonmagnetic system, can instead display long-range ferromagnetic or antiferromagnetic ordering, because of bridging oxo's that allow for superexchange and create unusually short Np···Np distances.[8] An explanation for this diametrically opposed behavior remains elusive. Np^{VI}, which is the simplest of these systems, is $5f^1$, and, sadly, examples of magnetic susceptibility measurements on these compounds are surprisingly rare.[4c] A different situation is encountered for Np^{IV} compounds. These compounds often display complex magnetism, because of the $5f^3$ electron configuration.[9] The Russell–Saunders approach predicts a $^4I_{9/2}$ ground state for Np^{IV}. However, intermediate coupling, configuration mixing, crystal field, and bonding effects all contribute to substantial deviations from the Russell–Saunders model in representing the wave function for this electron configuration. Actinide ions display magnetic behavior that is difficult to interpret, because of the unknown extent of hybridization, narrow bandwidths, and other factors that are discussed in depth in other articles and reviews since the 1970s.[10] There is not enough known about the magnetic complexities to fully understand the electronic structure of $5f^3$ compounds.[11]

The f-block selenites offer rich structural chemistry with a diversity of topologies for two reasons. First, there are a variety

Received: January 23, 2014
Published: June 25, 2014

   dx.doi.org/10.1021/ic500181t | Inorg. Chem. 2014, 53, 7154–7159

of Se^{IV} oxoanion species, found both in solution and in the solid state, that include $HSeO_3^-$, SeO_3^{2-}, and $Se_2O_5^{2-}$.[12] Second, these anions bind metal centers in a wide variety of modes. The most common selenite structural unit is the trigonal pyramidal SeO_3^{2-} anion, which possesses a stereochemically active lone-pair of electrons, and C_{3v} symmetry. The polarity of this anion makes it an attractive ligand for the development of nonlinear optical materials.[13] When this structural richness is combined with the unparalleled coordination variability of f-elements, the expectation is that these materials should display a vast array of new structure types, some of which may have atypical properties. The reactions of actinides with selenite have given rise to a series of compounds that include ostensibly simple combinations like Pu^{IV} selenite ($Pu(SeO_3)_2$),[11] as well as a much more complex mixed-valent systems such as the Np^{IV}/Np^{V} compound, $Np(NpO_2)_2(SeO_3)_3$.[14] More recently, several Np^{V} selenites were reported by Jin et al., and the magnetic behavior of these systems has proven to be quite rich.[15] The intricacies of the magnetism in these diverse neptunium selenites are proving to be difficult to comprehend, and our understanding of the electronic coupling in these compounds cannot yet be directly correlated or, more importantly, predicted based solely on structural features and site symmetry.

Herein, we report the synthesis, crystal structures, and absorption spectra of two new neptunium selenites: $Np(SeO_3)_2$ and $NpO_2(SeO_3)$. In addition, detailed magnetic susceptibility studies have been performed on $Np(SeO_3)_2$. The structure–property correlations found in $Np(SeO_3)_2$ extend the available examples of well-characterized 5f compounds, and assist in our understanding of magnetic coupling occurring in these systems.

EXPERIMENTAL SECTION

Syntheses. $^{237}NpO_2$ (99.9%, Oak Ridge), SeO_2 (99.4%, Alfa Aesar), and $Pb(NO_3)_2$ (99.9%, Alfa-Aesar) were used as received. Distilled water was used in all reactions. Reactions were run in Parr Model 4749 autoclaves with custom-made 10-mL polytetrafluoroethylene (PTFE) liners and metal jackets.

Caution! *^{237}Np ($t_{1/2}$ 2.14 × 10^6 years) represents a serious health risk, because of its α and γ emission, and especially because of its decay to the short-lived isotope ^{233}Pa ($t_{1/2}$ = 27.0 days), which is a potent β and γ emitter. All studies were conducted in a laboratory dedicated to studies on transuranium elements using procedures previously described.*[16]

$Np(SeO_3)_2$ and $NpO_2(SeO_3)$. NpO_2 (10.9 mg, 0.0405 mmol), SeO_2 (18.0 mg, 0.162 mmol), and $Pb(NO_3)_2$ (13.4 mg, 0.0405 mmol) were loaded in a 10-mL PTFE-lined autoclave, followed by the addition of 200 μL of water. The autoclave was sealed and placed in a furnace for 3 days at 200 °C. The box furnace was then cooled rapidly to 23 °C in 4 h. The product consisted of a colorless solution over brown prisms of $Np(SeO_3)_2$ and very large colorless prisms of $PbSeO_3$ with just a few large garnet-colored acicular crystals of $NpO_2(SeO_3)$. When the cooling rate was decreased to 5 °C/h from 200 to 23 °C, the yield of $NpO_2(SeO_3)$ increased to ∼20%. The majority of the solution was removed from the crystals, and water was added to keep the crystals under solution. The $Np(SeO_3)_2$ crystals were generally quite small and had a maximum volume of ∼0.04 mm^3, while $NpO_2(SeO_3)$ were approximately thrice this.

Crystallographic Studies. Single crystals of $Np(SeO_3)_2$ and $NpO_2(SeO_3)$ were mounted on Mitegen Mounts with viscous immersion oil and optically aligned on a Bruker D8 QUEST X-ray diffractometer. Initial intensity measurements were performed using an IμS X-ray source, a 50-W microfocused sealed tube (Mo Kα, λ = 0.71073 Å) with high-brilliance and high-performance focusing multilayer optics. Standard QUEST software was used for determination of the unit cells and data collection control. The intensities of reflections of a sphere were collected by a combination of four sets of exposures (frames). Each set had a different φ angle for the crystal, and each exposure covered a range of 0.5° in ω. A total of 1464 frames were collected with an exposure time per frame of 10–30 s, depending on the crystal. The SAINT software was used for data integration including Lorentz and polarization corrections. Semiempirical absorption corrections were applied using the program SADABS or TWINABS. Selected crystallographic information is listed in Table 1.

Table 1. Selected Crystallographic Data for $Np(SeO_3)_2$ and $NpO_2(SeO_3)$

	$Np(SeO_3)_2$	$NpO_2(SeO_3)$
formula mass	490.92	395.96
color	brown	garnet
habit	prism	acicular
space group	$P2_1/n$	$P2_1/m$
a (Å)	7.0089(5)	4.2501(3)
b (Å)	10.5827(8)	9.2223(7)
c (Å)	7.3316(5)	5.3840(4)
β (deg)	106.953(1)	90.043(2)
V (Å3)	520.18(6)	211.03(3)
Z	4	2
T (K)	100(2)	100(2)
λ (Å)	0.710 73	0.710 73
maximum θ (deg.)	27.540	27.560
ρ_{calcd} (g/cm^3)	6.269	6.231
μ (Mo Kα) (cm^{-1})	339.23	331.45
$R(F)$ for $F_o^2 > 2\sigma(F_o^2)^a$	0.0179	0.0373
$R_w(F_o^2)^b$	0.0410	0.1114

$^aR(F) = \sum||F_o| - |F_o||/\sum|F_o|$. $^bR_w(F_o^2) = [\sum[w(F_o^2 - F_c^2)^2]/\sum wF_o^4]^{1/2}$

Atomic coordinates and additional structural information are provided in the Supporting Information (CIFs). Because of the β angle being nearly 90°, crystals of $NpO_2(SeO_3)$ are pseudomerohedrally twinned, and this twinning creates pseudo-orthorhombic symmetry. The structure was solved in the monoclinic space group $P2_1/m$ with a suitable twin law and was checked for higher symmetry using PLATON.[17]

UV–vis–NIR Spectroscopy. UV-vis-NIR data were acquired from single crystals using a Craic Technologies microspectrophotometer. Crystals were placed on quartz slides under Krytox oil, and the data was collected from 200 nm to 1300 nm.

Magnetic Susceptibility Measurements. Magnetization measurements were conducted on 5.9 mg of polycrystalline $Np(SeO_3)_2$ using a Quantum Design superconducting quantum interference device (SQUID) magnetometer MPMS-XL. Zero-field-cooled (ZFC) and field-cooled (FC) measurements were performed under a constant direct-current (DC) magnetic field of 100 Oe over the temperature range of 1.8–300 K. The alternate-current (AC) magnetic susceptibility was measured under zero DC bias field in the temperature range of 1.8–4.2 K, with the frequency of AC field varied from 1 Hz to 1000 Hz. Isothermal field dependence of magnetization was measured with the magnetic field varying between 0 and 70 000 Oe at 1.8, 2.5, 10, 25, and 300 K. Hysteresis measurements were also performed at 1.8 K. The sample holders were measured separately under identical conditions, and their magnetic response was subtracted directly from the raw data. The intrinsic diamagnetic response of the sample was calculated using Pascal's constants and subtracted from the measured susceptibilities.[18]

RESULTS AND DISCUSSION

Synthesis. The hydrothermal reaction of NpO_2 with SeO_2, in the presence of $Pb(NO_3)_2$ generates two neptunium compounds with distinct structures and different oxidation states of the metal centers: $Np(SeO_3)_2$ and $NpO_2(SeO_3)$. It is

dx.doi.org/10.1021/ic500181t | Inorg. Chem. 2014, 53, 7154–7159

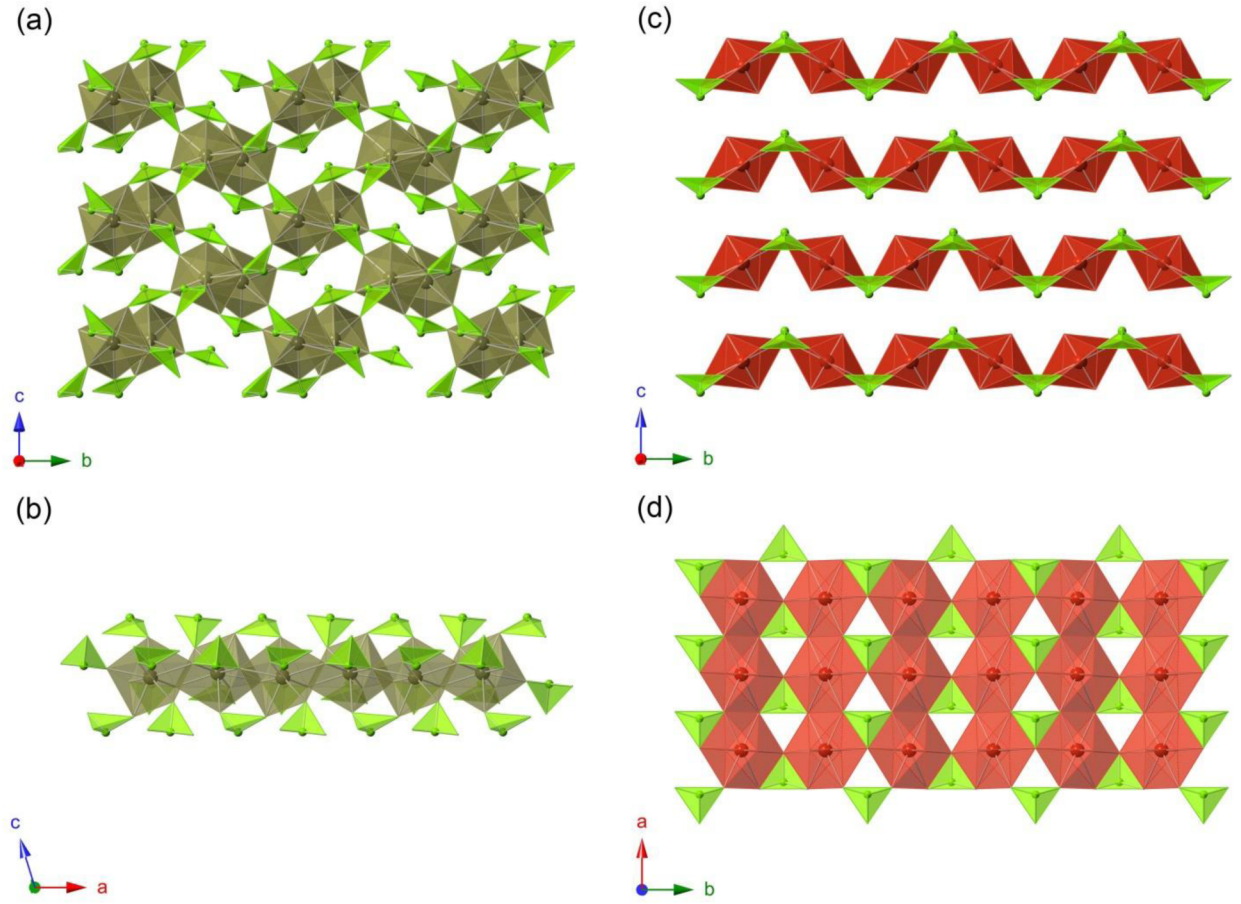

Figure 1. (a) View along the *a*-axis of part of the structure of $Np(SeO_3)_2$. (b) Chain of edge-sharing NpO_8 units extending along the *a*-axis; neptunium-containing polyhedra are shown in drab green, and the selenite units are shown in light green. (c) Layers of $NpO_2(SeO_3)$ stacking along the *c*-axis. (d) View of a $NpO_2(SeO_3)$ layer in the [*ab*] plane; neptunium polyhedra are shown in garnet, and the selenite structural units are shown in light green.

important to note that, if $Pb(NO_3)_2$ is removed, $NpO_2(SeO_3)$ forms as the major product. $Pb(NO_3)_2$ is playing two key roles. First, the Pb^{2+} ions are removing some of the selenite anions from solution by forming $PbSeO_3$. Second, we have demonstrated, on several occasions, that nitrate is highly redox active with actinides under hydrothermal conditions.[19] Np^V is often erroneously considered to be the only viable oxidation state for neptunium in water with dissolved oxygen; this is a conjecture that is largely based on the standard reduction potentials that predict the comproportionation of Np^{IV} and Np^{VI} to yield Np^V. However, numerous studies have demonstrated that low pH, high concentration, high temperatures, and strong complexants all dramatically alter this equilibrium such that well-characterized Np^{IV}, Np^V, and Np^{VI} products, as well as several mixed-valent compounds, have all been isolated.[4c,20] Furthermore, we have shown in many systems that hydrothermal conditions are reducing for neptunium, and Np^{IV} products often result from hydrothermal reactions.[4c] The formation of both products are readily explained on this basis. The reaction probably occurs via oxidization and solubilization of NpO_2 to yield Np^V that undergoes subsequent disproportionation. The expected low solubility of $Np(SeO_3)_2$ removes the Np^{IV} from solution, shifting the equilibrium. The Np^{VI} produced from this same reaction is reduced, and the end result is that only a few crystals of the Np^{VI} product are isolated, and $Np(SeO_3)_2$ is the major product. In other words, the isolation of the Np^{IV} compound, $Np(SeO_3)_2$, as the major product can be largely attributed to a solubility-driven mechanism. Quenching the reaction leads to an almost exclusive formation of $Np(SeO_3)_2$.

STRUCTURES AND TOPOLOGICAL DESCRIPTIONS

Structure of $Np(SeO_3)_2$. Single-crystal X-ray diffraction (XRD) reveals that the structure of $Np(SeO_3)_2$ is isotypic with that of $Ce(SeO_3)_2$[21] and $Pu(SeO_3)_2$.[11] It crystallizes in the centrosymmetric, monoclinic space group $P2_1/n$. It features a dense three-dimensional framework, constructed from Np-oxo chains bridged by SeO_3^{2-} ions (Figure 1a). The metal-oxo chains consist of edge-sharing NpO_8 units extending along the *a*-axis, as shown in Figure 1b. In determining which polyhedron the eight-coordinate Np site most closely approximates, we used an algorithm described by Raymond and co-workers.[22] These calculations demonstrate that the geometry for the NpO_8 unit is best described as a bicapped trigonal prism (C_{2v}, S = 13.11°). However, the coordination environment is highly distorted, and it is also close to being approximated by a D_{2d} trigonal dodecahedron (S = 13.89°). There are small channels in the structure that extend down the *a*-axis in which the lone-pairs of electrons from the selenite anions reside. Selected bond distances for $Np(SeO_3)_2$ are given in Table 2. The Np−O bond distances range from 2.256(5) Å to 2.520(4) Å. The SeO_3^{2-} oxoanion adopt the standard trigonal pyramid geometry with approximate C_{3v} symmetry. Se−O bonds range from 1.681(5)

dx.doi.org/10.1021/ic500181t | Inorg. Chem. 2014, 53, 7154−7159

Table 2. Selected Bond Distances for $Np(SeO_3)_2$ and $NpO_2(SeO_3)$

$Np(SeO_3)_2$		$NpO_2(SeO_3)$	
bond	distance (Å)	bond	distance (Å)
Np(1)−O(1)	2.520(4)	Np(1)−O(1)	1.737(9)
Np(1)−O(1)	2.378(4)	Np(1)−O(1)′	1.737(9)
Np(1)−O(2)	2.2694(4)	Np(1)−O(2)	2.405(10)
Np(1)−O(3)	2.405(4)	Np(1)−O(2)′	2.405(10)
Np(1)−O(3)	2.356(5)	Np(1)−O(2)″	2.485(10)
Np(1)−O(4)	2.334(5)	Np(1)−O(2)‴	2.485(10)
Np(1)−O(5)	2.277(4)	Np(1)−O(3)	2.599(7)
Np(1)−O(6)	2.256(5)	Np(1)−O(3)′	2.599(7)
Se(1)−O(2)	1.694(5)	Se(1)−O(2)	1.693(9)
Se(1)−O(5)	1.698(4)	Se(1)−O(2)′	1.693(9)
Se(1)−O(6)	1.681(5)	Se(1)−O(3)	1.706(14)
Se(2)−O(1)	1.732(4)		
Se(2)−O(3)	1.713(4)		
Se(2)−O(4)	1.673(4)		

Å to 1.698(4) Å for Se(1), and from 1.673(4) Å to 1.732(4) Å for Se(2), which are the typical distances for Se−O bonds. Despite none of the building blocks of $Np(SeO_3)_2$ being on inversion centers, the structure is still centrosymmetric with the inversion centers located between Np ions. Bond-valence sums (BVS) were calculated using bond distances determined from the bond distance data and predetermined bond-valence parameters for the Np ions. The optimized bond valence parameters R_0 = 1.972 and b = 0.538 were utilized in calculating bond valence for Np^{IV} based on 19 known Np^{IV} structures.[23] This set of parameters give a BVS of 4.01 v.u. for Np^{IV} ions, indicating the tetravalent nature of the Np^{IV} ions in $Np(SeO_3)_2$.

Structure of $NpO_2(SeO_3)$. This compound forms a lamellar structure consisting of neptunyl ions (NpO_2^{2+}) and SeO_3^{2-} trigonal pyramids, as shown in Figure 1c. The lone pair of electrons on the selenite ligands, which are directed into the interstitial space, are pointing in alternating directions along the c-axis, as indicated by the centrosymmetric space group. All three of the selenite O atoms bridge between two Np sites and are, therefore, μ_3-O atoms. Within each layer, the Np polyhedra share two edges along the a-axis and two corners along the b-axis with each other (Figure 1d). A consequence of this is that the Np···Np distances are greater along the b-axis than along the a-axis. The NpO_2^{2+} cations are coordinated by six O atoms in the equatorial plane to form a NpO_8 hexagonal bipyramidal geometry. Selected bond distances for $NpO_2(SeO_3)$ are given in Table 2. The two axial Np≡O bond distances of the neptunyl unit are 1.738(9) Å, whereas the equatorial Np−O bond distances range from 2.404(9) Å to 2.599(7) Å. It is interesting to note that, even though all of the oxo atoms from the selenite anions are μ_3-oxo's, the equatorial Np−O bond distances vary significantly. This is simply attributed to whether they reside at the vertex being used for corner-sharing or edge-sharing between the NpO_8 polyhedra. Se−O bonds range from 1.693(9) Å to 1.70(1) Å; these bonds are provided in Table 2. The site symmetry in this compound is quite interesting, because the neptunium center resides on an inversion site, and the Se atom resides on a mirror. The combination of these site symmetries allows for four O2 atoms to be generated in the equatorial plane of neptunium from a single crystallographically unique oxygen site. The site symmetry of the neptunium also has the potential for having significant effects on its spectroscopic features (*vide infra*). Coordination enviroments are depicted in Figure 2.

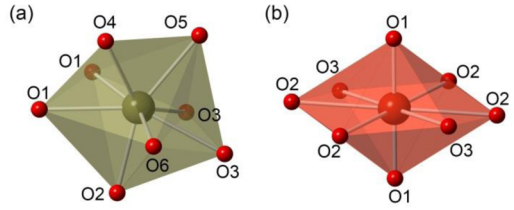

Figure 2. Coordination environments of the neptunium centers: (a) the eight-coordinate Np^{IV} site in $Np(SeO_3)_2$ is best described as a bicapped trigonal prism; (b) the Np^{VI} site in $NpO_2(SeO_3)$ has a hexagonal bipyramidal geometry.

Using bond valence parameters, R_0 = 2.025 and b = 0.444, BVS calculations were performed for Np^{VI} according to 23 known Np^{VI} structures and yield an average BVS of 5.90 v.u. for Np^{VI} ions in $NpO_2(SeO_3)$.[23]

Magnetic Properties of $Np(SeO_3)_2$. The magnetic susceptibility (χ) of $Np(SeO_3)_2$ was measured in the ZFC and FC modes in the temperature range of 1.8−200 K with an applied DC magnetic field of 100 Oe (see Figure 3a). The temperature dependence of χT reveals a large temperature-independent component, χ_{TIP} (Figure 3a, inset). This indicates that, in addition to the J = 9/2 ground state of the Np^{IV} ion, there is a significant population of the higher-lying J-manifolds of excited states, which leads to the strong deviation from the Curie−Weiss law. The temperature dependence of the ZFC and FC magnetic susceptibility shows an abrupt increase at lower temperatures, regardless of whether the sample was field-cooled. A comparison of the ZFC and FC susceptibility curves reveals a bifurcation at ∼3 K (see Figure 3a). The Curie temperature, T_C = 3.1(1) K, was estimated as the point of the maximum absolute value of $d\chi_{FC}/dT$. The occurrence of magnetic phase transition at this temperature was further confirmed by an examination of AC magnetic susceptibility that revealed a frequency-independent maximum in the temperature dependence of χ' (Figure 3b). The lack of frequency dependence discards the possibility of spin-glass behavior.

Magnetization measurements conducted at 1.8 K revealed that $Np(SeO_3)_2$ behaves as a soft ferromagnet with negligible hysteresis (Figure 3c). Nevertheless, the field-dependent magnetization does not saturate, even at 7 T, and the maximum value achieved, 0.8 μ_B, is much lower than expected for the ground state of the Np^{IV} ion (3.6 μ_B). These observations suggest the possibility of weak ferromagnetism, i.e., in the magnetically ordered state the Np^{IV} moments are not exactly collinear, but show some tilting. Such ordering can be caused by the presence of different magnetic exchange constants operating along and between the chains. For example, a stronger ferromagnetic intrachain coupling and a weaker antiferromagnetic interchain coupling can lead to the canted ferromagnetic ordering of Np^{IV} magnetic moments.

UV-vis-NIR Spectroscopy. The oxidation states of the Np ions in $Np(SeO_3)_2$ and $NpO_2(SeO_3)$ were further confirmed by UV-vis-NIR absorption spectroscopy, as shown in Figure 4. Np^{IV} characteristic absorption features consist of a series of Laporte-forbidden f−f transitions, which were assigned many years ago.[24] The transitions observed for $Np(SeO_3)_2$ are consistent with Np^{IV}.[4a,24,25] For Np^{VI}, the $5f^1$ electron configuration typically yields a single somewhat broad

dx.doi.org/10.1021/ic500181t | Inorg. Chem. 2014, 53, 7154−7159

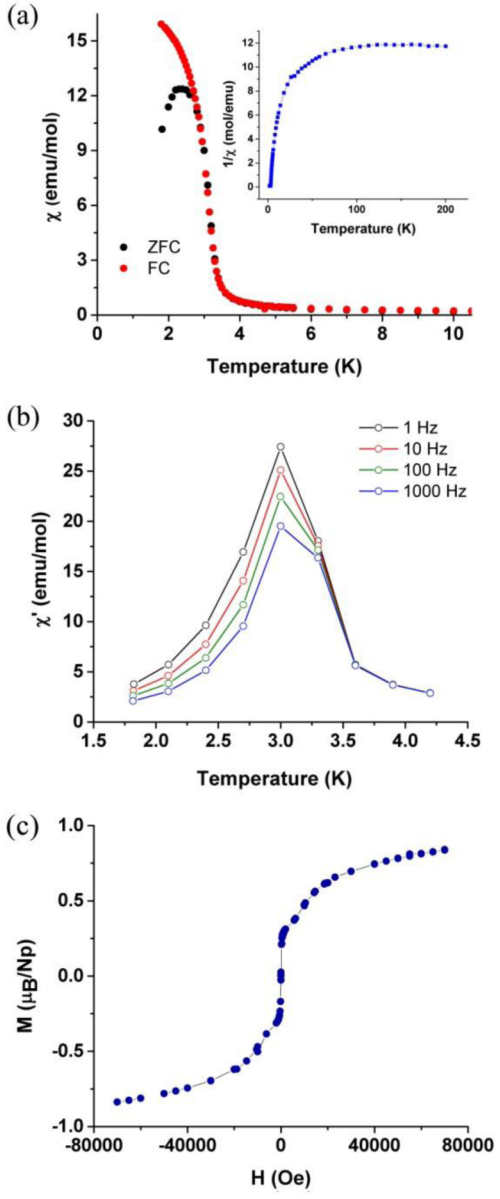

Figure 3. Magnetic properties of $Np(SeO_3)_2$: (a) the temperature dependence of zero-field-cooled (ZFC) and field-cooled (FC) DC magnetic susceptibility measured at 100 Oe (inset shows the temperature dependence of $1/\chi$, showing the large temperature-independent paramagnetic contribution); (b) the temperature dependence of AC magnetic susceptibility measured at various frequencies of the applied AC field and zero DC bias field; and (c) isothermal field dependence of magnetization measured at 1.8 K.

Laporte-forbidden f–f transition in the NIR region near 1150 nm. It is interesting to note that when Np^{VI} resides on an inversion center (or any f-element in any oxidation state) that the selection rules are more strictly enforced, and the f–f transitions *can* be entirely absent. Rao and co-worker, have referred to this as "silent" neptunium in the case of Np(V).[26] In $NpO_2(SeO_3)$, the neptunium center is on an inversion center, and yet the f–f transition is still observed. There has been considerable speculation over the years that the broadness of the transition at 1150 nm, may be indicative that it is not a pure f–f transition and may involve 5f/6d mixing. If this is the case, the transition would be allowed, regardless of the site symmetry. The distinct peak observed at 1000 nm may be

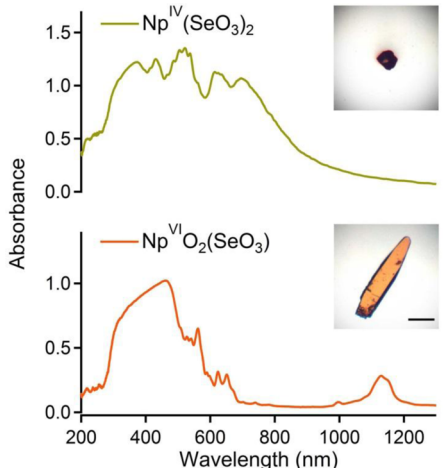

Figure 4. UV-vis-NIR spectra of $Np(SeO_3)_2$ and $NpO_2(SeO_3)$ at 298 K, along with an image of the crystal that was analyzed.

indicative of Np^V, which could be present within our crystals in trace amounts.[27] This peak has also been observed in other formally Np^{VI} compounds such as $NpO_2[B_8O_{11}(OH)_4]$.[23] Additional higher energy vibronically coupled charge-transfer bands, which are also allowed transitions, were observed from 450 nm to 650 nm for Np^{VI}. These features are all consistent with a Np^{VI} compound.[28]

CONCLUSIONS

Two neptunium selenites containing neptunium in different oxidation states, $Np^{IV}(SeO_3)_2$ and $Np^{VI}O_2(SeO_3)$, were prepared from the same reaction via the disproportionation of Np^V, where the ratio of products can be controlled via cooling rate. Absorption spectroscopy and bond-valence sums support these oxidation-state assignments. Magnetic susceptibility measurements yield an ordering temperature of 3.1(1) K. The $\chi_M T$ vs T plot (Figure 3a, inset) reveals strong TIP effects that are evident in the large deviation observed from the expected Curie–Weiss plot throughout the entire temperature range. The strong moment (Figure 3a) coupled with nearly no observed magnetic hysteresis lead us to conclude that the crystals are behaving as a soft ferromagnetic material. In addition, we assume there to be an antiferromagnetic component of the magnetic exchange between the Np ions, because of the low near-saturation moment of 0.8 μ_B at our maximum field of 7 T.

ASSOCIATED CONTENT

Supporting Information

Crystallographic information has been provided as Supporting Information (CIF files). This material is available free of charge via the Internet at http://pubs.acs.org.

AUTHOR INFORMATION

Corresponding Author

*Tel.: 850-645-0477. E-mail: albrecht-schmitt@chem.fsu.edu.

Notes

The authors declare no competing financial interest.

ACKNOWLEDGMENTS

We are grateful for support provided by the Chemical Sciences, Geosciences, and Biosciences Division, Office of Basic Energy Sciences, Office of Science, Heavy Elements Chemistry

Program, U.S. Department of Energy (under Grant No. DE-FG02-13ER16414).

REFERENCES

(1) (a) Edelstein, N. M.; Fuger, J.; Morss, L. R. *The Chemistry of the Actinide and Transactinide Elements*; Springer: Dordrecht, The Netherlands, 2010. (b) Cotton, S. *Lanthanide and Actinide Chemistry*; Wiley: Chichester, U.K., 2006.
(2) (a) Moiseev, I. V.; Kuperman, A. Y.; Borodina, N. N.; Vinokurov, V. A. *Radiokhimiya* **1975**, *17*, 189−195. (b) Shilov, V. P. *Radiokhimiya* **1980**, 727−732. (c) Sarsfield, M. J.; Taylor, R. J.; Maher, C. J. *Radiochim. Acta* **2007**, *95*, 677−682.
(3) (a) Wang, S.; Villa, E. M.; Diwu, J.; Alekseev, E. V.; Depmeier, W.; Albrecht-Schmitt, T. E. *Inorg. Chem.* **2011**, *50*, 2527−2533. (b) Meredith, N. A.; Polinski, M. J.; Lin, J.; Simonetti, A.; Albrecht-Schmitt, T. E. *Inorg. Chem.* **2012**, *51*, 10480−10482.
(4) (a) Diwu, J.; Wang, S.; Liao, Z.; Burns, P. C.; Albrecht-Schmitt, T. E. *Inorg. Chem.* **2010**, *49*, 10074−10080. (b) Villa, E. M.; Wang, S.; Alekseev, E. V.; Depmeier, W.; Albrecht-Schmitt, T. E. *Eur. J. Inorg. Chem.* **2011**, *2011*, 3749−3754. (c) Bray, T. H.; Nelson, A.-G. D.; Jin, G. B.; Haire, R. G.; Albrecht-Schmitt, T. E. *Inorg. Chem.* **2007**, *46*, 10959−10961.
(5) Gal, J.; Kroup, M.; Hadari, Z. *Solid State Commun.* **1976**, *19*, 73−74.
(6) Jin, G.-B.; Skanthakumar, S.; Haire, R. G.; Soderholm, L.; Ibers, J. A. *Inorg. Chem.* **2011**, *50*, 1084−1088.
(7) (a) Bullock, J. I.; King, M. E. *J. Chem. Soc., Dalton Trans.* **1975**, 1360−1364. (b) Arnold, P. L.; Potter, N. A.; Magnani, N.; Apostolidis, C.; Griveau, J.-C.; Colineau, E.; Morgenstern, A.; Caciuffo, R.; Love, J. B. *Inorg. Chem.* **2010**, *49*, 5341−5343.
(8) Magnani, N.; Colineau, E.; Eloirdi, R.; Griveau, J. C.; Caciuffo, R.; Cornet, S. M.; May, I.; Sharrad, C. A.; Collison, D.; Winpenny, R. E. P. *Phys. Rev. Lett.* **2010**, *104*, 197203.
(9) Liu, Y.; Liu, Y.; Liu, B. *J. Chem. Educ.* **2010**, *88*, 295−298.
(10) (a) Masset, A. C.; Michel, C.; Maignan, A.; Hervieu, M.; Toulemonde, O.; Studer, F.; Raveau, B.; Hejtmanek, J. *Phys. Rev. B* **2000**, *62*, 166−175. (b) Jensen, M. P.; Bond, A. H. *J. Am. Chem. Soc.* **2002**, *124*, 9870−9877.
(11) Bray, T. H.; Skanthakumar, S.; Soderholm, L.; Sykora, R. E.; Haire, R. G.; Albrecht-Schmitt, T. E. *J. Solid State Chem.* **2008**, *181*, 493−498.
(12) Mao, J.-G.; Jiang, H.-L.; Kong, F. *Inorg. Chem.* **2008**, *47*, 8498−8510.
(13) (a) Jiang, H.-L.; Xie, Z.; Mao, J.-G. *Inorg. Chem.* **2007**, *46*, 6495−6501. (b) Ling, J.; Albrecht-Schmitt, T. E. *Inorg. Chem.* **2007**, *46*, 5686−5690. (c) Lee, D. W.; Ok, K. M. *Inorg. Chem.* **2013**, *52*, 5176−5184.
(14) Almond, P. M.; Sykora, R. E.; Skanthakumar, S.; Soderholm, L.; Albrecht-Schmitt, T. E. *Inorg. Chem.* **2004**, *43*, 958−963.
(15) Jin, G. B.; Skanthakumar, S.; Soderholm, L. *Inorg. Chem.* **2012**, *51*, 3220−3230.
(16) Albrecht-Schmitt, T. E.; Almond, P. M.; Sykora, R. E. *Inorg. Chem.* **2003**, *42*, 3788−3795.
(17) Spek, A. L. *J. Appl. Crystallogr.* **2003**, *36*, 7.
(18) Bain, G. A.; Berry, J. F. *J. Chem. Educ.* **2008**, *85*, 532−536.
(19) (a) Wang, S.; Alekseev, E. V.; Depmeier, W.; Albrecht-Schmitt, T. E. *Chem. Commun.* **2010**, *46*, 3955−3957. (b) Wang, S.; Alekseev, E. V.; Miller, H. M.; Depmeier, W.; Albrecht-Schmitt, T. E. *Inorg. Chem.* **2010**, *49*, 9755−9757.
(20) (a) Bray, T. H.; Ling, J.; Choi, E. S.; Brooks, J. S.; Beitz, J. V.; Sykora, R. E.; Haire, R. G.; Stanbury, D. M.; Albrecht-Schmitt, T. E. *Inorg. Chem.* **2007**, *46*, 3663−3668. (b) Gruen, D. M.; Hutchison, C. A., Jr. *J. Chem. Phys.* **1954**, *22*, 386−393.
(21) Maeno, Y.; Hashimoto, H.; Yoshida, K.; Nishizaki, S.; Fujita, T.; Bednorz, J. G.; Lichtenberg, F. *Nature* **1994**, *372*, 532−534.
(22) Gorden, A. E. V.; Xu, J.; Raymond, K. N.; Durbin, P. *Chem. Rev.* **2003**, *103*, 4207−4282.
(23) Wang, S. A.; Villa, E. M.; Diwu, J. A.; Alekseev, E. V.; Depmeier, W.; Albrecht-Schmitt, T. E. *Inorg. Chem.* **2011**, *50*, 2527−2533.
(24) (a) Hagan, P. G.; Cleveland, J. M. *J. Inorg. Nucl. Chem.* **1966**, *28*, 2905−2909. (b) Kepert, D. L. Aspects of the Stereochemistry of Eight-Coordination. In *Progress in Inorganic Chemistry*; John Wiley & Sons, Inc.: Hoboken, NJ, 2007; pp 179−249.
(25) Cotton, F. A.; Torralba, R. C. *Inorg. Chem.* **1991**, *30*, 2196−2207.
(26) Tian, G.; Rao, L.; Oliver, A. *Chem. Commun.* **2007**, 4119−4121.
(27) Fedoseev, A. M.; Gogolev, A. V.; Shilov, V. P. *Radiochemistry* **2013**, *55*, 155−157.
(28) Liu, G.; Wang, S.; Albrecht-Schmitt, T. E.; Wilkerson, M. P. *J. Phys. Chem. A* **2012**, *116*, 8297−8302.